

Detection and Fundamental Applications of Individual First Galaxies

Renyue Cen¹

ABSTRACT

First galaxies formed within halos of mass $M = 10^{7.5} - 10^9 M_{\odot}$ at $z = 30 - 40$ in the standard cold dark matter (CDM) universe may each display an extended hydrogen 21-cm absorption halo against the cosmic microwave background with a brightness temperature decrement of $\delta T = -(100 - 150)$ mK at a radius $0.3 \leq r \leq 3.0$ comoving Mpc, corresponding to an angular size of $10 - 100$ arcseconds. A 21-cm tomographic survey in the redshift shell $z = 30 - 40$ (at $35 - 45$ MHz), which could be carried out by the next generation of radio telescopes, is expected to be able to detect millions of first galaxies and may prove exceedingly profitable in enabling (at least) four fundamental applications for cosmology and galaxy formation. First, it may yield direct information on star formation physics in first galaxies. Second, it could provide a unique and sensitive probe of small-scale power in the standard cosmological model hence physics of dark matter and inflation. Third, it would allow for an independent, perhaps “cleaner” characterization of interesting features on large scales in the power spectrum such as the baryonic oscillations. Finally, possibly the most secure, each 21-cm absorption halo is expected to be highly spherical and faithfully follow the Hubble flow. By applying the Alcock-Paczyński test to a significant sample of first galaxies, one may be able to determine the dark energy equation of state with an accuracy likely only limited by the accuracy with which the matter density can be determined independently.

Subject headings: galaxies - radio - intergalactic medium - cosmology: theory

1. Introduction

It is of wide interest to detect and understand the first generation of galaxies, expected to form in the redshift range $z = 30 - 50$ in the standard CDM universe (Spergel et al. 2003).

¹Princeton University Observatory, Princeton University, Princeton, NJ 08544; cen@astro.princeton.edu

Extensive literatures on 21-cm properties of neutral hydrogen in the dark ages and during cosmological reionization have long focused on large-scale fluctuations of the intergalactic neutral hydrogen and global spectral features (e.g., Hogan & Rees 1979; Scott & Rees 1990). In this *Letter* we point out a unique feature possessed by the first *individual* galaxies of mass $10^{7.5} - 10^9 M_\odot$ formed at $z = 30 - 40$ — a large hydrogen 21-cm absorption halo against the cosmic microwave background (CMB). Each 21-cm absorption halo has a size $10'' - 100''$ with a brightness temperature decrement of $\delta T = -(100 - 150)$ mK at $35 - 45$ MHz, which could serve as a visible proxy for each galaxy that otherwise may be undetectable. The next generation of radio telescopes, such as LOFAR, may be able to detect such a signal. A range of fundamental applications is potentially possible with a redshift (i.e., 21-cm tomographic) survey of the first galaxies in the redshift shell $z = 30 - 40$, which may hold the promise to revolutionize the field of cosmology and shed illuminating light on dark matter, dark energy and inflation physics. Throughout, a standard (Wilkinson Microwave Anisotropy Probe) WMAP-normalized Λ CDM model is used (unless indicated otherwise): $\Omega_M = 0.31$, $\Lambda = 0.69$, $\Omega_b = 0.048$, $H_0 = 69$ km/s/Mpc, $n_s = 0.99$ and $\sigma_8 = 0.90$.

2. Large 21-cm Absorption Halos of First Galaxies

A first-generation galaxy is expected to emit UV and X-ray radiation, each carving out an H II region of size (ignoring recombination): $r_{\text{HII}} \sim 43 \left(\frac{M_h}{10^7 M_\odot}\right)^{1/3} \left(\frac{c_*}{0.1}\right)^{1/3} \left(\frac{f_{esc}}{0.1}\right)^{1/3} \left(\frac{N_p}{8 \times 10^4}\right)^{1/3}$ kpc comoving, where M_h is the halo mass, c_* the star formation efficiency, f_{esc} the ionizing photon escape fraction into the intergalactic medium (IGM), and N_p the number of hydrogen ionizing photons produced by each baryon formed into stars, ($\sim 10^{4.5-5}$ for a massive metal-free Population III IMF; Bromm, Kudritzki, & Loeb 2001). Hard X-ray photons (≥ 1 keV) produced escape deep into the IGM with a distance of $\sim 500 - 1000$ comoving megaparsecs, building an X-ray background. Sandwiched between small H II regions and the X-ray sea sits a quite large Ly α scattering region (Loeb & Rybicki 1999), resulting in a four-layer structure, as depicted in Figure 1.

The IGM in the vicinity of a galaxy interacts with ionizing UV and soft X-ray as well as near Ly α photons emanating from the galaxy, which can be computed. The most important and relevant physical processes are (1) the interaction between neutral gas and near Ly α photons emitted by the central host galaxy, which couples the spin temperature of the IGM to its kinetic temperature (Wouthuysen 1952; Field 1958), and (2) the interaction between neutral gas and ionizing UV and soft X-ray photons emanating from the host galaxy, which provides a heating source for the otherwise cold IGM up to some small radius. In the absence of heating the kinetic temperature T_k of the IGM would be equal to

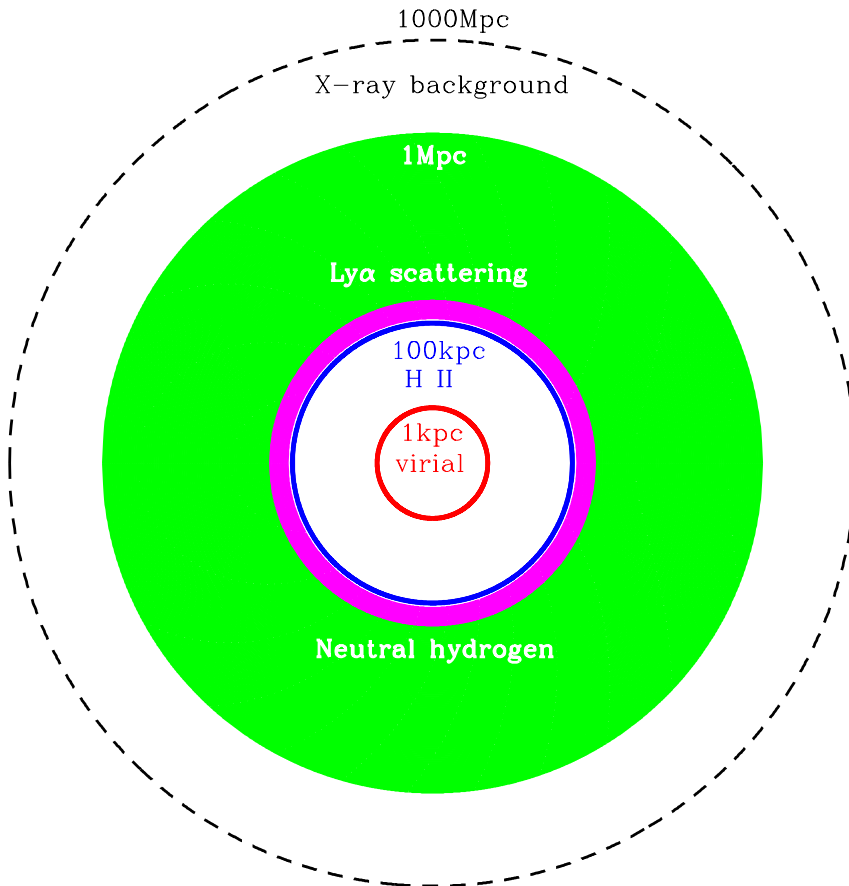


Fig. 1.— shows a four-layer structure around an individual galaxy at very high redshift. The inner-most central region (inside the red circle) is the virialized region where star formation occurs with a typical size of about 1 kpc comoving. The next region, enclosed by the blue circle, is the ionized region with a typical size of order 40 – 200kpc comoving. Exterior to the ionized region lies the Ly α scattering region shown in magenta for the inner (heated) part and in green for the outer (cold) part, where Ly α photons can strongly couple the 21-cm spin temperature to the kinetic temperature of the gas; the inner part shown in magenta is significantly heated by UV and soft X-ray photons emanating from the host galaxy, while most of the region shown in green remains cold at a temperature set by the general IGM. Outside the green circle is the general IGM that is only affected collectively by cumulative X-ray background (as well as a Ly α background), as symbolically circumscribed by the dashed black circle.

$T_{\text{IGM}} \approx 18 \left(\frac{1+z}{31}\right)^2$ K (for the redshift range of interest here) since beginning of decoupling with CMB at $z \sim 200$ (Peebles 1993). We perform spherically the transfer of UV and soft X-ray radiation from the host galaxy outward to compute (1) the development of the HII region around the galaxy as a function of time, (2) the evolution of the temperature of the surrounding IGM, subject to UV and soft X-ray heating by the host galaxy, as a function of radius and time, and (3) the Ly α coupling coefficient y_α as a function of radius and time.

We assume a uniform IGM density equal to the mean gas density of the universe (i.e., $\Delta = 0$ in equation 1 below). Two scenarios of metal-free star formation in first galaxies are considered: (1) all stars have a single mass of $200 M_\odot$ (VMS), advocated by Oh et al. (2001) and Qian & Wasserburg (2002), and (2) an IMF has the Salpeter slope of 2.35 with a lower cutoff of $25 M_\odot$ and an upper cutoff of $120 M_\odot$ (SAL), close to what favored by Umeda & Nomoto (2003), Tumlinson, Venkatesan, & Shull (2004) and Tan & McKee (2004). We adopt the library of stellar spectra and ages from Schaerer (2002); we use a black-body radiation spectrum for each star of chosen mass with an effective surface temperature from Table 3 of Schaerer (2002) but slightly adjusted so as to produce the correct ratio of the number of photons above helium II Lyman limit to the number of photons above hydrogen Lyman limit, averaged over the lifetime of each star (see Table 4 of Schaerer 2002). We use an escape fraction for Lyman limit photons f_{esc} from the host galaxy and self-consistently a frequency dependent escape fraction for other UV and soft X-ray photons assuming that they are subject to the same absorbing column in the galaxy. All escaped photons (emerging from the virial radius) are then subject to the (time-dependent) combined absorption of H I, He I and He II in the IGM, self-consistently computed. Since the Ly α scattering region is mostly neutral with a residual ionized fraction of 2×10^{-4} left from recombination (Peebles 1993), we assume that $\eta = 14\%$ of X-ray energy is used to heat the gas (Shull & Van Steenberg 1985) with the heating rate per hydrogen atom at radius r computed with the following formula: $\frac{dE}{dt} = \int_0^\infty \frac{\eta L_\nu}{4\pi h\nu r^2} (\sigma_\nu(HI)(h\nu - h\nu_H) + \xi\sigma_\nu(HeI)(h\nu - h\nu_{HeI}) + \xi\sigma_\nu(HeII)(h\nu - h\nu_{HeII})) e^{-\tau_\nu} d\nu$, where L_ν is the luminosity per unit frequency of the galaxy; ν_{HI} , ν_{HeI} and ν_{HeII} are ionization potentials of H, He I and He II, respectively; $\sigma_\nu(HI)$, $\sigma_\nu(HeI)$ and $\sigma_\nu(HeII)$ are photo-ionization cross-sections of H, He I and He II, respectively; ξ is ratio of helium number density to hydrogen number density; τ_ν is the optical depth from the galaxy to radius r at frequency ν .

The spin temperature of neutral hydrogen (Field 1958, 1959) is then given by $T_S = \frac{T_{\text{cmb}} + y_\alpha T_k + y_c T_k}{1 + y_\alpha + y_c}$, where $y_c \equiv \frac{C_{10}}{A_{10}} \frac{T_*}{T_k}$ is the collisional coupling coefficient with the collisional de-excitation rate $C_{10} = \frac{4}{4} \kappa(1 - 0)n_H$, $\kappa(1 - 0)$ taken from Zygelman (2005), n_H is the mean hydrogen density and $T_* = 0.0682$ K is the hydrogen hyperfine energy splitting.

In the expression for the Ly α coupling coefficient $y_\alpha = \frac{P_{10}T_s}{A_{10}T_k}$, $A_{10} = 2.87 \times 10^{-15} \text{ s}^{-1}$ is spontaneous emission coefficient of the 21-cm line, the indirect de-excitation rate P_{10} of the hyperfine structure levels is related to the total Ly α scattering rate P_α by $P_{10} = 4P_\alpha/27$ (Field 1958). Here $P_\alpha = \int F_\nu \sigma(\nu) d\nu$ with F_ν being the Ly α photon flux (in units of $\text{cm}^{-2} \text{ s}^{-1}$) and $\sigma(\nu) = \sigma_\alpha \phi(\nu) = \frac{3}{8\pi} \lambda_\alpha^2 A_\alpha \phi(\nu)$ being the cross section for Ly α scattering (MMR), where $\lambda_\alpha = 1.216 \times 10^{-5} \text{ cm}$ is the wavelength of the Ly α line, $A_\alpha = 6.25 \times 10^8 \text{ s}^{-1}$ is the spontaneous Einstein coefficient for Ly α line and $\phi(\nu)$ is the normalized Ly α line (Voigt) profile with $\int \phi(\nu) d\nu = 1$. Most of the Ly α scattering is accomplished by UV photons slightly on the blue side of the Ly α that redshift into Ly α resonant line due to the Hubble expansion (note that $\Delta\nu/\nu \sim 10^{-3}$ due to Hubble expansion at $r \sim 1\text{Mpc}$ comoving), not the intrinsic Ly α line photons that escape from the host galaxy and redshift to the damping wing (Madau, Meiksin, & Rees 1997; MMR). Additional physical processes that were not treated previously, including higher-order Lyman lines that result in cascade in two-photon emission, fine structure of Ly α resonance and spin-flip scattering, introduce corrections of order unity to P_α (CM; Hirata 2005; Chuzhoy & Shapiro 2005) but all these corrections terms are insignificant for our case, and we only apply the relatively large correction term S_c (~ 1.5) as shown in Figure 4 of CM due to a spectral shape change near Ly α . The observed brightness temperature increment/decrement against the CMB is

$$\delta T = 41(1 + \Delta)x_H \left(\frac{T_s - T_{\text{cmb}}}{T_s}\right) \left(\frac{\Omega_b h^2}{0.02}\right) \left(\frac{0.15}{\Omega_M h^2}\right)^{1/2} \left(\frac{1+z}{31}\right)^{1/2} \text{ mK}, \quad (1)$$

where Δ is gas overdensity relative to the mean, x_H neutral hydrogen fraction, $T_{\text{cmb}} = 2.73(1+z)$ K CMB temperature and other symbols have their usual meanings.

Figure 2 shows the profile of δT for four cases of halo masses with each choice of IMF. Let us examine each of the four regions (sketched in Figure 1) with respect to 21-cm observations. Inside the virial radius (the red circle in Figure 1) the gas is overdense with $\delta \geq 100$ and a positive large-amplitude emission signal may result, if a significant amount of neutral hydrogen gas exists within. However, the size of this regions falls below $0.1''$ and its signal is unlikely to be detectable in the foreseeable future. The H II region (inside the blue circle in Figure 1) is ionized hence $\delta T = 0$. In the region outside the Ly α scattering region (exterior to the green region in Figure 1) the spin temperature of the IGM has been progressively attracted to the temperature of the CMB with gradually weakening coupling to the gas kinetic temperature by atomic collisions, producing a small but non-negligible 21-cm absorption signal at the redshift of interest ($z \sim 30 - 40$) (Loeb & Zaldarriaga 2004).

It is the Ly α scattering region that is of most interest here. In the inner part of the Ly α scattering region (shown in magenta in Figure 1) the IGM is significantly heated by UV and soft X-ray photons to exceed the CMB temperature, while its spin temperature

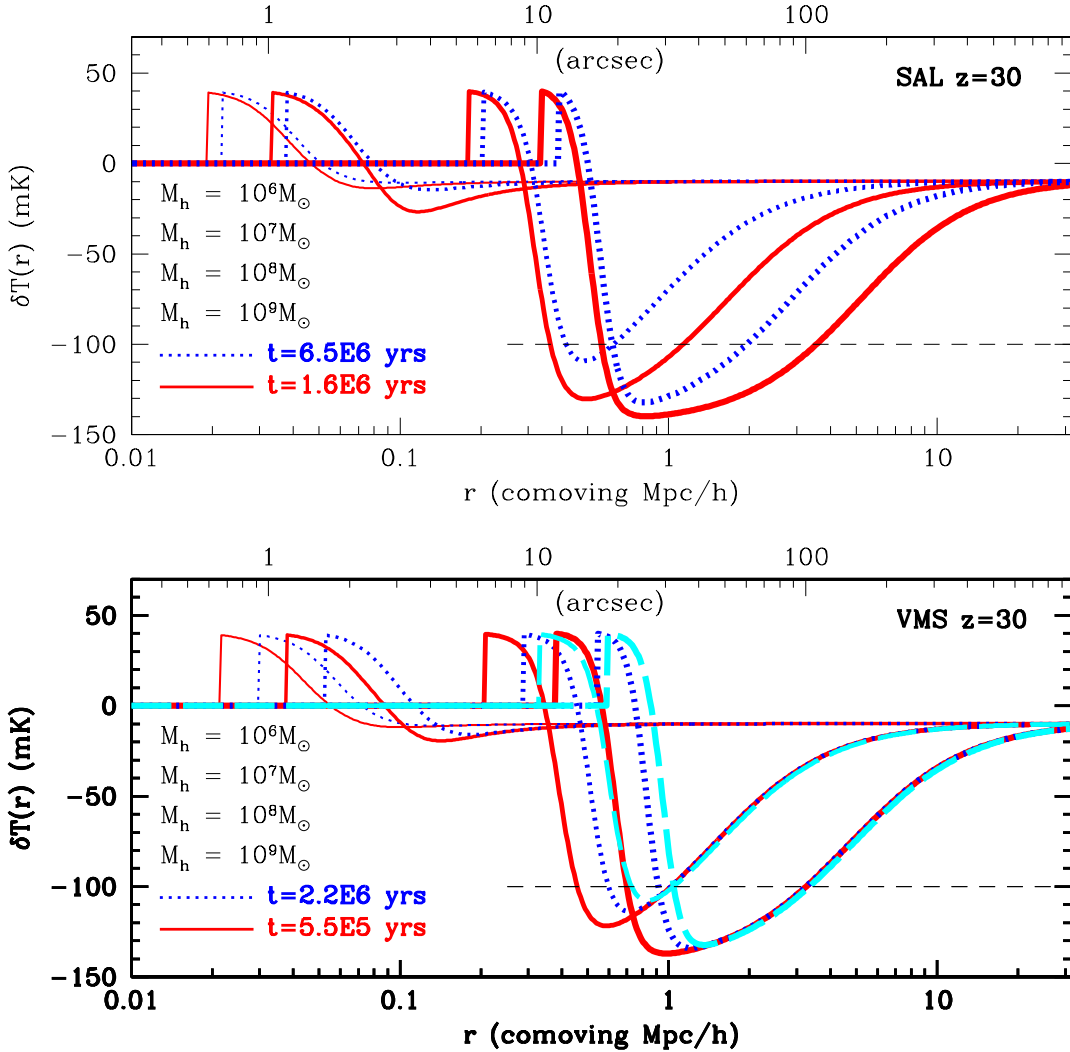


Fig. 2.— The top panel shows the δT profiles for halos with $M_h = (10^6, 10^7, 10^8, 10^9) M_\odot$, respectively, from top to bottom, at $z = 30$ as a function of comoving radius, with the adopted SAL IMF (SAL, see text). The top x-axis is in units of arcseconds. The division mass between large halos and minihalos at $z = 30$ is $\sim 1.4 \times 10^7 M_\odot$. For each chosen value of M_h two snapshots are shown, at $t = 1.6 \times 10^6$ yrs (solid curves) and $t = 6.5 \times 10^6$ yrs (dotted curves), where $t = 6.5 \times 10^6$ yrs is the lifetime of the least massive stars with $M = 25 M_\odot$ in the chosen SAL IMF. The bottom panel is similar to the top panel but for the adopted VMS IMF, and the two snapshots are at $t = 5.5 \times 10^5$ yrs (solid curves) and $t = 2.2 \times 10^6$ yrs (dotted curves), where $t = 2.2 \times 10^6$ yrs is the lifetime of the stars with $M = 200 M_\odot$. Also shown as two long-dashed curves in the bottom panel are two cases for $M_h = (10^8, 10^9) M_\odot$, respectively, with soft X-ray ($h\nu > 100$ eV) intensity artificially boosted by a factor of 10, which should be compared to the respective cases shown as blue curves located slightly to their left. The star formation efficiency is assumed to be 0.10 for large halos and 0.001 for minihalos (Abel et al. 2002). Escape fraction $f_{esc} = 0.01$ is used, although the results depend very weakly on it.

is very strongly coupled to its kinetic temperature by Ly α scattering. As a result, the inner radial region at 0.01 – 0.04 Mpc/h comoving for minihalos and 0.04 – 0.4 Mpc/h comoving for large halos displays an emission signal against CMB with an amplitude of $\delta T \sim 30$ mK (a shark dorsal fin-like feature in Figure 2). Going outward (shown in green in Figure 1), the soft X-ray heating abates (because the cumulative optical depth to these photons increases quickly) but the Ly α scattering remains strong, up to a distance of about 10 Mpc/h comoving. Consequently, a strong 21-cm absorption signal against the CMB with an amplitude of $\delta T = -(100 - 150)$ mK at $\sim 35 - 45$ MHz (for $z = 30 - 40$) on a scale of 0.3 – 3 Mpc/h comoving, corresponding to an angular scale of $10'' - 100''$, is produced for large halos. This is the 21-cm absorption halo — a unique and strong feature for the large first galaxies. We note that the absorption signal cast by minihalos (the two top sets of thin curves in each panel in Figure 2) is relatively weak due to a combination of low mass and low star formation efficiency. We will therefore focus on large halos for practical observability purposes.

Besides stars, no other soft X-ray source in the galaxy is assumed to concurrently exist. We shall examine the validity of this assumption in detail. The density of the interstellar medium plays an important role for some of the potentially relevant processes considered here and it is assumed to be $n(z) = n_0(1+z)^3$, where local interstellar density $n_0 = 1 \text{ cm}^{-3}$. This assumption should hold in hierarchical structure formation model for the following reasons. The mean gas density scales as $(1+z)^3$ and halos at low and high redshift in cosmological simulations show similarities when density and length are measured in their respective comoving units (e.g., Navarro, Frenk, & White 1997; Del Popolo 2001). The spin parameters (i.e., angular momentum distribution) of both high and low redshift halos have very similar distributions peaking at a nearly identical value $\lambda \sim 0.05$ (Peebles 1969; White 1984; Barnes & Efstathiou 1987; Ueda et al. 1994; Steinmetz & Bartelmann 1995; Cole & Lacey 1996; Bullock et al. 2001). Thus, cooling gas in galaxies at low and high redshift should collapse by a similar factor before the structure becomes dynamically stable (e.g., rotation support sets in), resulting in interstellar densities scaling as $(1+z)^3$. Direct simulations (Abel et al. 2002; Bromm et al. 2002) suggest a gas density of $10^3 - 10^4 \text{ cm}^{-3}$ by the end of the initial free fall for minihalos at $z \sim 20$, verifying this simple analysis.

We will estimate each of several possible types of soft X-ray emission sources in turn. First, let us estimate soft X-ray emission from supernova remnants. Assuming the standard cooling curve (Sutherland & Dopita 1993) we find that at $z = 30$ a supernova blastwave with an initial explosion energy of 5×10^{52} erg (for a star of mass $200 M_\odot$; e.g., Heger & Woosley 2002) would enter its rapid cooling phase at a temperature of 2.7×10^7 K. This implies that the energy emitted at $\sim 100 - 300$ eV from the cooling shell is about 7%. A $200 M_\odot$ mass would release 2.5×10^{54} erg total energy due to nuclear burning, out

of which 0.3% is released in photons at 100 – 300eV for our adopted radiation spectrum. Therefore, the ratio of total photon energy from the supernova remnant to that from the star is 0.4 – 0.5. Thus, for the VMS IMF, stellar soft X-ray appears to dominate over that from its supernova remnant. The soft X-ray contribution from supernova remnant cooling increases relatively compared to that from the star itself with decreasing stellar mass and we estimate that the overall contribution from the two components may become comparable for the SAL IMF case, averaged over time. Second, we will examine X-rays produced from cooling of supernova-accelerated relativistic electrons by CMB photons via inverse Compton (IC) process (e.g., Oh 2001). For adiabatic shocks, as is appropriate in our case, the IC spectral energy distribution has a two-power-law form: $L_\nu \propto \text{constant}$ at $E < E_{break}$ and $L_\nu \propto \nu^{-1}$ at $E > E_{break}$. The break energy is $E_{break} = 70$ keV, independent of redshift with the assumed scaling of the interstellar medium density with redshift. Then the ratio of energy from IC to that from stars is found to be $10^{-4} - 10^{-3}$ in the 100 – 300eV band, depending on the exact upper energy cutoff (assuming 10% of supernova explosion energy is utilized to accelerate relativistic electrons in shocks). Clearly, contribution to soft X-rays from IC process is unimportant. Third, X-ray binaries during the relatively short lifetime of massive stars may be rare, for top-heavy IMFs of concern here. We can make an estimate based on the calculation by Rappaport, Podsiadlowski & Pfahl (2005), who give an ultra luminous X-ray binary formation rate of 3×10^{-5} per supernova. It is clear that even if each X-ray binary is able to release as much energy as in a supernova explosion itself and all in the soft X-ray band, the resulting contribution will be less than a fraction of a percent of that from stars. Fourth, stellar mass black holes (BH) of $\sim 10 - 100 M_\odot$ may be produced in significant numbers with a top-heavy IMF as well as a central galactic BH. It seems that stellar BH accretion is likely significantly suppressed and small due to feedback effect from stars on surrounding gas (e.g., Mori, Umemura, & Ferrara 2004; Alvarez, Bromm, & Shapiro 2005). A concomitant contribution of soft X-rays from central BH accretion in the lifetime of a $200 M_\odot$ star is approximately $(M_{BH}/M_*) \times (1/0.007) \times (t_*/t_E) \times (f_{BH,SX}/f_{*,SX}) = 0.6 f_{BH,SX} (M_{BH}/M_*/0.003)$, after inserting soft X-ray emission fraction for a $200 M_\odot$ stellar spectrum of $f_{*,SX} = 0.003$, stellar lifetime $t_* = 2.2 \times 10^6$ yrs and Eddington time $t_E = 4.4 \times 10^8$ yrs, where $f_{BH,SX}$ is the energy fraction released by the BH accretion in the soft X-ray band (100 – 300eV). Thus, if the ratio of black hole mass to (bulge) stellar mass follows the local Magorrian (Magorrian et al. 1998) relation, then, unless most of the accretion energy is released in the soft X-ray band, contribution from central BH accretion to the soft X-ray band is relatively small. Fifth, thermal bremsstrahlung emission from gravitational shock heated gas is likely negligible due to a low gas temperature ($T \sim 10^4$ K). Finally, soft X-rays from massive first stars themselves are thought to be produced by stellar winds and quite uncertain. Recent work suggests that the winds hence soft X-ray emission from metal-free stars are expected

to be insignificant (e.g., Krticka & Kubat 2005). In summary, soft X-rays from neglected, possible sources other than that from the stellar photospheres would, at most, make a modest correction to what is adopted in our calculation. To ascertain our conclusion, we compute a case with the amplitude of soft X-ray intensity at $h\nu \geq 100$ eV artificially raised by a factor of 10 and do not find any significant effect that would qualitatively change our results (Figure 2). The reason is that the IGM quickly becomes optically thick to a few 100eV soft X-ray photons at ~ 1 Mpc comoving. Therefore, our results should be quite robust.

Since we are concerned with gas of relatively low temperature ~ 20 K, heating by a cumulative (hard) X-ray background may become relevant at some redshift. We estimate when this may happen in the CDM model. While an X-ray background may be generated by a variety of processes, black hole accretion at the centers of galaxies are thought to be the most dominant (e.g., Ricotti & Ostriker 2003; Kuhlen & Madau 2005), estimated as follows. Let us suppose the energy extraction efficiency from black accretion is α and a fraction f_x of the released energy is in the form of hard X-rays. Then, the X-rays may collectively heat up the IGM temperature at most (ignoring Compton cooling and assuming all X-ray photons in the background are consumed by the IGM) by an increment

$$\Delta T_{\text{xray}} = 1.1 \left(\frac{f_{\text{coll}}}{10^{-6}} \right) \left(\frac{c_*}{0.1} \right) \left(\frac{\alpha}{0.1} \right) \left(\frac{M_{\text{BH}}/M_*}{0.003} \right) \left(\frac{f_x}{0.029} \right) \text{ K} \quad (2)$$

(assuming 14% of X-ray energy is used to heat the IGM; Shull & Van Steenberg 1985), where f_{coll} is the fraction of matter that has collapsed to halos where stars have formed. Under the reasonable assumption that the parameters have their adopted fiducial values (for α see Yu & Tremaine 2002, f_x see Elvis et al. 1994, for c_* see Gnedin 2000), it becomes evident that, for the very first galaxies formed in the universe that comprise a collapsed mass fraction less than 10^{-6} , heating of the IGM by an X-ray background radiation field may be small. Figure 3 shows cumulative halo mass functions at redshift $z = (20, 30, 40)$, based on Press-Schechter (1974) formalism (using $\delta_c = 1.67$ and the standard model of Spergel et al. 2003), which should be accurate for the exponentially falling regime of interest here (Sheth & Tormen 1999; Jenkins et al. 2001). Figure 3 suggests that at redshift $z \geq 30$ heating of the IGM by an X-ray background is small. Neglected contributions to the X-ray background from other sources (X-ray binaries, supernova remnants, etc) (e.g., Oh 2001, Cen 2003) will likely just add a modest numerical correction factor for equation (2) and the net effect, if any, would push the epoch for significant heating by an X-ray background to a slightly higher redshift (note that structure formation is exponentially increasing with decreasing redshift at $z = 30 - 40$). But even a factor of a few upward correction to equation (2) would still leave the temperature of IGM $z = 30$ relatively unaffected by an X-ray background.

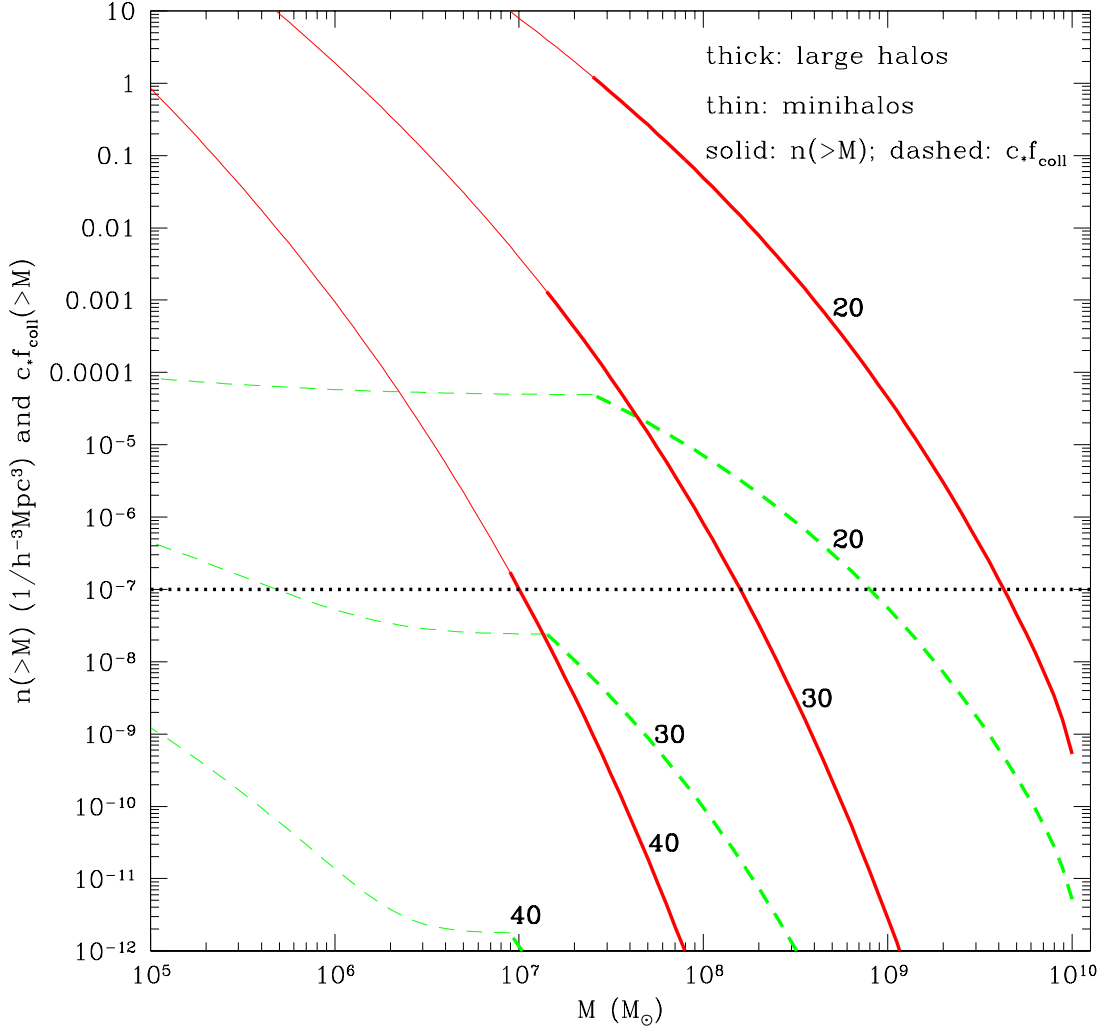


Fig. 3.— shows cumulative halo mass functions (solid curves) at redshift $z = (20, 30, 40)$, respectively, from top to bottom. Each solid curve is broken into two parts with a thick portion corresponding to large halos with efficient atomic cooling and a thin portion corresponding to minihalos with molecular cooling only. The corresponding dashed curves are cumulative $c_* f_{\text{coll}}$ for the three cases, assuming star formation efficiency of $c_*(\text{large}) = 0.1$ for large halos and of $c_*(\text{mini}) = 0.001$ for minihalos (Abel et al. 2002). The horizontal dotted line indicates $c_* f_{\text{coll}} = 10^{-7}$ (see equation 2).

Another critical issue is whether heating of IGM by Ly α photons is important. In a recent accurate calculation based on Fokker-Planck approximation, Chen & Miralda-Escudé (2004; CM) show that the heating rate by Ly α photons is much lower than previous estimates (MMR). We recast their important result (equation 17 of CM and using Figure 3 of CM), the heating rate per hydrogen atom and per Hubble time, β , in the following way:

$$\beta \equiv \frac{\Gamma_c}{Hn_Hk_B} = 0.08\left(\frac{P_\alpha}{P_{th}}\right) \text{ K} \quad (3)$$

at $z = 30$, where k_B is the Boltzmann constant, H is the Hubble constant and $P_{th} = 2.4 \times 10^{-11}(\frac{1+z}{31}) \text{ s}^{-1}$ is the thermalization rate for Ly α scattering at $z = 30$, above which Ly α scattering brings down the spin temperature to the gas kinetic temperature (MMR). The Hubble time is 1.4×10^8 yrs at $z = 30$. So, over the duration of a stellar lifetime 6×10^6 yrs (of the least massive stars in our model, $25 M_\odot$), the gas will be heated up by 0.003 K at $\frac{P_\alpha}{P_{th}} = 1$. For the regime of interest where we see the strong 21-cm absorption signal (Figure 2) we find $\frac{P_\alpha}{P_{th}} = 1 - 10$. Thus, heating of surrounding IGM by Ly α photons emanating from the host galaxy can be safely neglected. In addition, since we are concerned with early times when the universe is far from being ionized and the number of Ly α photons per hydrogen atom is significantly less than unity, indicating that heating by the background Ly α photons can also be safely neglected (CM). Furthermore, heating rate by high order Lyman series photons is still lower and thus negligible (Pritchard & Furlanetto 2005).

3. Fundamental Applications

We have demonstrated a unique feature of first galaxies. A large 21-cm survey of the first galaxies will be invaluable. Demanding that each of the physical quantities be resolved by a factor of 10 would translate to the following requirements: an angular resolution of $\sim 1''$, a spectral resolution of $\sim 4\text{kHz}$ ($\Delta\nu \sim 40\text{kHz}$ across a radius of $1\text{Mpc}/h$ at $z = 30$ due to the Hubble expansion) and a sensitivity of $\sim 10 \text{ mK}$ at $35 - 45 \text{ MHz}$. Among the next generation of radio telescopes currently under construction/consideration, LOFAR (<http://www.lofar.org>) appears to be best positioned to be able to carry out such a survey, at least for some of the brighter and larger galaxies. LOFAR is currently designed to reach a frequency as low as 10MHz with an angular resolution of $3'' - 4''$ at $35 - 45\text{MHz}$, a sensitivity of 10 mK and a spectral resolution (i.e., processing capability) of 1 kHz (e.g., Rottgering 2003), while MWA (<http://web.haystack.mit.edu/arrays/MWA/index.html>), PaST (<http://web.phys.cmu.edu/~past/index.html>) and SKA (<http://www.skatelescope.org>) appear to be placed out of the $35 - 45\text{MHz}$ range, as they stand now.

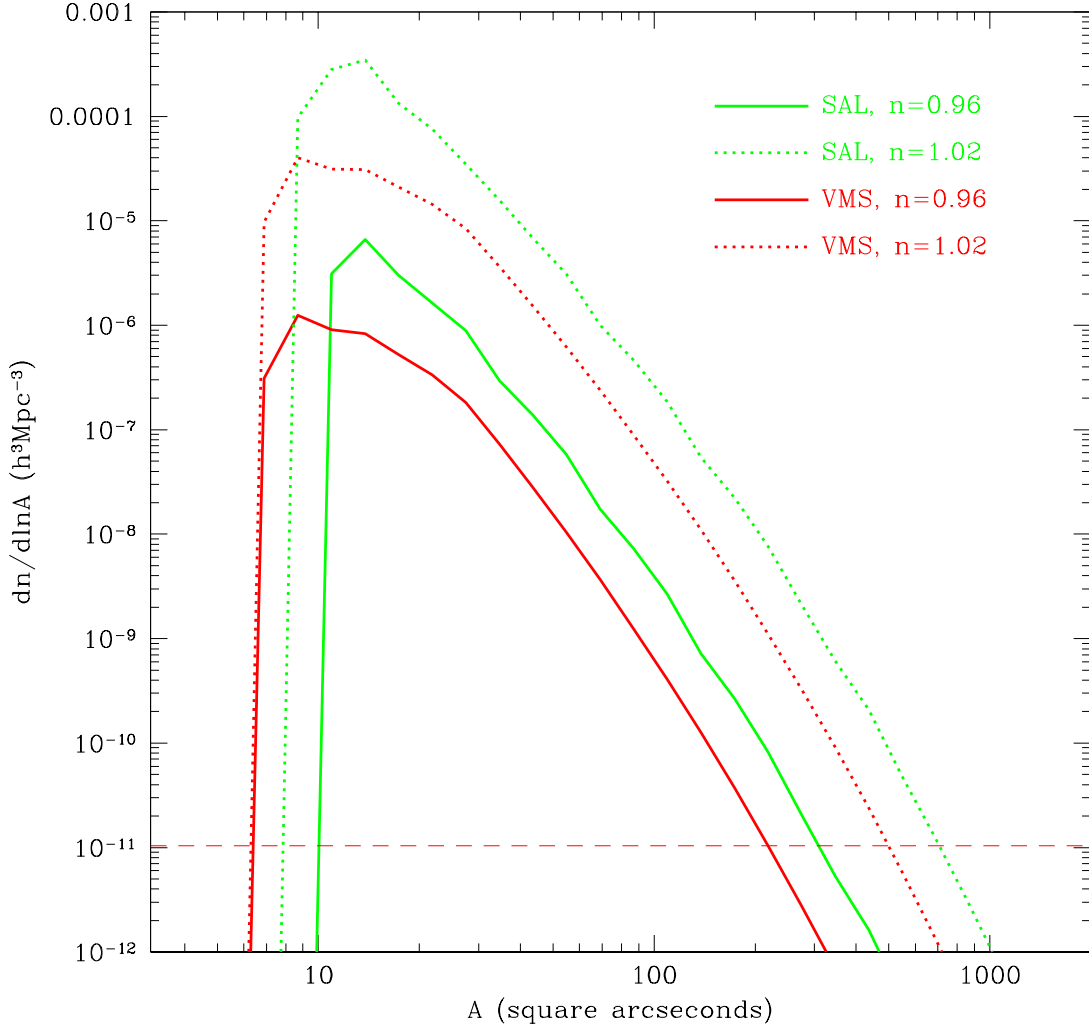


Fig. 4.— shows the density of galaxies versus the maximum absorption cross section (i.e., in the plane of the large circle centered on the galaxy perpendicular to the line of sight) with $\delta T < -100$ mK at $z = 3$ in the standard LCDM model except the index of the power spectrum n_s , for which two values are chosen, $n_s = 0.96$ (solid curve) and $n_s = 1.02$ (dotted curve), possibly bracketing its likely range. Two cases for two IMF are shown with the thick curves for SAL and the thin curves for VMS. The density is computed taking into account the time variations of stellar radiation spectra and finite lifetime. The horizontal dashed curve indicates the density with which the volume of the redshift shell $z = 28$ to $z = 32$ would contain one such object.

Figure 4 shows the density of galaxies versus the maximum absorption cross section (i.e., in the plane of the large circle centered on the galaxy perpendicular to the line of sight) with $\delta T < -100$ mK. Here we point out four fundamental and potentially ground-breaking applications regarding cosmology and galaxy formation, if a 21-cm tomographic survey of galaxies in the redshift shell $z = 30 - 40$ is carried out, which may be able to detect millions of galaxies.

First, a characteristic sharp fall-off at $5 - 10$ square arcseconds and a characteristic peak of the number of 21-cm absorption halos is expected, as seen in Figure 4 due to a lower star formation efficiency in (and low mass of) minihalos, as suggested by available simulations (Abel et al. 2002). This should yield direct information on physics of cooling and star formation in first galaxies, which may be unobtainable otherwise by any other means in the foreseeable future. Note that the left cutoff and the peak density are functions of c_* and $g(\text{IMF})$ (noting the differences between SAL and VMS cases in Figure 4), where $g(\text{IMF})$ denotes dependence on the properties of IMF such as stellar lifetime and spectrum. A full parameter space exploration will be given in a separate paper with more detailed treatments. We expect that c_* and $g(\text{IMF})$ may be determined separately, when jointly analyzed with the density of absorption halos in the context of the standard CDM model.

Second, we see that the density of strong 21-cm absorption halos depends strongly on n_s , as testified by the large difference (a factor of ~ 50) between solid and dotted curves in Figure 4. One may then obtain a constraint on n_s , which is made possible because the effect due to difference in IMF may be isolated out, as discussed above, thanks to the features in the density of absorption halos (e.g., peak location and sharp fall-off at the low end). Let us estimate a possible accuracy of such measurements. At $n \sim 10^{-6} h^3 \text{Mpc}^{-3}$ one would find 0.1 million galaxies in the redshift shell between $z = 28$ and $z = 32$, giving a relative fraction (Poisson) error of 0.3%. By comparing the solid and dotted curves in Figure 4, we find that a constraint on n_s with $\Delta n_s = 0.01$ ($\sim 3\sigma$) may be achieved. This may have the potential to discriminate between inflationary theories (e.g., Liddle & Lyth 1992; Peiris et al. 2003). In addition, the constraint placed on the temperature (or mass) of dark matter particles or running of the spectral index may be still tighter, because a significant, finite dark matter temperature or a running index tends to suppress small-scale power exponentially thus amplify the effects. The high-sensitivity constraint on small-scale power is afforded by the physical fact that we are dealing with rare $\geq 5 - 6\sigma$ peaks in the matter distribution.

Third, clustering of galaxies may be computed using such a survey containing potentially hundred of thousands to millions of galaxies in a comoving volume of size $\sim 100 \text{Gpc}^3$ (for the redshift shell $z = 28 - 32$). Both the survey volume and the number

of observable galaxies within are large enough to allow for accurate determinations of the correlations of first galaxies, particularly on large scales. It may then provide an independent, perhaps “cleaner” characterization of interesting features in the power spectrum such as the baryonic oscillations, with the advantage that they are not subject to subsequent complex physical processes, including cosmological reionization, gravitational shock heating of the IGM and complex interplay between galaxies and IGM, which in turn might introduce poorly understood biases in galaxy formation. A comparison between clustering of first galaxies and local galaxies (e.g., Eisenstein et al. 2005) will provide another, high-leverage means to gauge gravitational growth and other involved processes between $z = 30$ to $z = 0$.

Finally, the scale ($\sim 1\text{Mpc}$ comoving) of the 21-cm absorption halo signals is much greater than the nonlinear scale and virial radius (both $\sim 1\text{kpc}$ comoving). Thus, the IGM region in the 21-cm absorption halo is expected to closely follow the Hubble flow. Since near $\text{Ly}\alpha$ photons (between $\text{Ly}\alpha$ and $\text{Ly}\beta$) are not subject to absorption by hydrogen (and helium) atoms whose distribution might be complex, they escape into the IGM in a spherical fashion. Additionally, since the dependence on Δ is linear (see equation 2), density inhomogeneities are likely to average out (to zero-th order) and results do not depend sensitively on uncertain linear density fluctuations in the IGM. Although there might exist “pores” in the domain of 21-cm absorption halo due to fluctuations in local IGM temperatures which may be caused by local shock heating due to formation of minihalos, the overall effect is likely negligible, because the mass fraction contained in all halos down to a mass as small as $M_h = 10^5 M_\odot$ is about 10^{-4} at $z = 30$. Furthermore, at $n = 10^{-6} h^3 \text{Mpc}^{-3}$ the mean separation between the galaxies is $100 \text{Mpc}/h$, much larger than the size of $\text{Ly}\alpha$ scattering regions of size $\sim 1\text{Mpc}/h$, so overlapping of the latter should be very rare (taking into account the known fact that they are strongly clustered in the standard cosmological model with *gaussian* random fluctuations; Mo & White 1996). For these reasons, each 21-cm absorption halo is expected to be highly spherical in real space. Therefore, 21-cm absorption halos are ideal targets to apply the Alcock-Paczyński (1979) test. Accurate measurements of angular size $\Delta\theta$ and radial depth Δv for a sample of galaxies would yield a sample of $d_A(z)H(z)$, where $d_A(z)$ and $H(z)$ are the angular diameter distance and Hubble constant, respectively, both of which are, in general, functions of Ω_M , $w(\equiv p/\rho)$ and k , with w describing the equation of state for dark energy and k being the curvature of the universe. As an example, let us assume that $\Omega_M(\approx 0.3)$ has been fixed exactly by independent observations and $k = 0$ and that $w \approx -1$. Then one obtains $|d\ln[d_A(z)H(z)]/dw| = 0.45$ at $z = 30$ (Huterer & Turner 2001). Let us suppose a relative measurement error on each individual $d_A(z)H(z)$ is 20%, then with ten thousand galaxies, one could obtain a highly accurate constraint on w with $\Delta w = 20\%/0.45/\sqrt{10000} \sim 0.004$.

Likely, the accuracy of w determined by this method may eventually be limited by the accuracy with which Ω_M (and k) can be determined by independent observations, due to the degenerate nature. We stress that this method is valid for each individual first galaxy and unaffected by uncertainties, for example, in the precise abundance of such galaxies.

In post-survey analyzes one faces the practical issue of extracting the wanted signals from the raw data, whose amplitude is expected to be dominated by foreground radio sources, including galactic synchrotron radiation, galactic and extragalactic free-free emission, and extragalactic point sources (e.g., Di Matteo, Ciardi, & Miniati 2004). While seemingly daunting, it has already been shown that signals of the amplitude proposed here may be recovered with relatively high fidelity, when one takes into account the expected, potent differences in the spectral and angular properties between the 21-cm signal and foreground contaminants (e.g., Zaldarriaga, Furlanetto, Hernquist 2004; Santos, Cooray, & Knox 2005; Wang et al. 2005). Since the 21-cm absorption halos are expected to be rather regular and simple, one might be able to significantly enhance the signal by using additional techniques, such as matched filter algorithm, in combination with foreground “cleaning” methods. Finally, the amount of data in such a high spatial and frequency resolution 3-dimensional survey will be many orders of magnitude larger than that of WMAP. Computational challenges for analyzing it will be of paramount concern and most likely demand new and innovative approaches.

4. Conclusions

It is shown that a first galaxy hosted by a halo of mass $M = 10^{7.5} - 10^9 M_\odot$ at $z = 30 - 40$ possesses a large 21-cm absorption halo against the CMB with a brightness temperature decrement $\delta T = -(100 - 150)$ mK and an angular size of $10'' - 100''$. A 21-cm tomographic survey of galaxies in the redshift shell at $z = 30 - 40$ may detect millions of galaxies and may yield critical information on cosmology and galaxy formation. A successful observation may need an angular resolution of $\leq 1''$, a spectral resolution of ≤ 4 kHz, and a sensitivity of ≤ 10 mK at 35 – 45 MHz. LOFAR appears poised to be able to execute this unprecedented task, at least for the high end of the distribution.

At least four fundamental applications may be launched with such a survey, which could potentially revolutionize cosmological study and perhaps the field of astro-particle physics. First, it may provide unprecedented constraint on star formation physics in first galaxies, for there is a proprietary sharp feature related to the threshold halo mass for efficient atomic cooling. Second, it may provide a unique and sensitive probe of the small-scale power in the cosmological model hence physics of dark matter and inflation, by being able to, for

example, constrain n_s to an accuracy of $\Delta n_s = 0.01$ at a high confidence level. Constraints on the nature of dark matter particles, i.e., mass or temperature, or running of index could be still tighter. Third, clustering of galaxies that may be computed with such a survey will provide an independent set of characterizations of potentially interesting features on large scales in the power spectrum including the baryonic oscillations, which may be compared to local measurements (Eisenstein et al. 2005) to shed light on gravitational growth and other involved processes from $z = 30$ to $z = 0$. Finally, the 21-cm absorption halos are expected to be highly spherical and trace the Hubble flow faithfully, and thus are ideal systems for an application of the Alcock-Paczyński test. Exceedingly accurate determinations of key cosmological parameters, in particular, the equation of state of the dark energy, may be finally realized. As an example, it does not seem excessively difficult to determine w to an accuracy of $\Delta w \sim 0.01$, if Ω_M has been determined to a high accuracy by different means. If achieved, it may have profound ramifications pertaining dark energy and fundamental particle physics (e.g., Upadhye, Ishak, & Steinhardt 2005).

If a null detection of the proposed signal is found, as it might turn out, implications may be as profound. It might be indicative of some heating and/or reionizing sources in the early universe ($z = 30 - 200$) that precede or are largely unrelated to structure formation, possibly due to yet unknown properties of dark matter particles or dark energy. Alternatively, star formation and/or BH accretion in first galaxies may be markedly different from our current expectations.

I thank Dr. Daniel Schaerer for helpful information on Pop III stars. This research is supported in part by grants AST-0206299, AST-0407176 and NAG5-13381.

REFERENCES

- Abel, T., Bryan, G.L., & Norman, M.L., 2002, *Science*, 295, 93
- Alcock, C., & Paczyński, B. 1979, *Nature*, 281, 358
- Alvarez, M, Bromm, V., & Shapiro, P.R. 2005, astro-ph/0507684
- Barnes, J., & Efstathiou, G. 1987, *ApJ*, 319, 575
- Bromm, V., Coppi, P.S., & Larson, R.B. 2002, *ApJ*, 564, 23
- Bromm, V., Kudritzki, R.P., & Loeb, A. 2001, *ApJ*, 552, 464

- Bullock, J.S., Dekel, A., Kolatt, T.S., Kravtsov, A.V., Klyping, A.A., Porciani, C., & Primack, J.R. 2001, *ApJ*, 555, 240
- Cen, R. 2003, *ApJ*, 591, 12
- Chen, X., & Miralda-Escudé, J. 2004, *ApJ*, 602, 1 (CM)
- Chuzhoy, L., & Shapiro, P.R. 2005, astro-ph/0512206
- Cole, S., & Lacey, C. 1996, *MNRAS*, 281, 716
- Del Popolo, A. 2001, *MNRAS*, 325, 1190
- Di Matteo, T., Ciardi, B., & Miniati, F. 2004, *MNRAS*, 355, 1053
- Eisenstein, D.J., et al. 2005, *ApJ*, 633, 560
- Elvis, M., et al. 1994, *ApJS*, 95, 1
- Field, G.B. 1958, *Proc. IRE*, 46, 240
- Field, G.B. 1959, *ApJ*, 129, 551
- Gnedin, N.Y. 2000, *ApJ*, 535, L75
- Heger, A., & Woosley, S.E. 2002, *ApJ*, 567, 532
- Hirata, C.M. 2005, astro-ph/0507102
- Hogan, C.J., & Rees, M.J. 1979, *MNRAS*, 188, 791
- Huterer, D., & Turner, M.S. 2001, *Phys. Rev. D.* 64, 123527
- Jenkins, A., et al. 2001, *MNRAS*, 321, 372
- Krticka, J., & Kubat, J. 2005, astro-ph/0509171
- Kuhlen, M., & Madau, P. 2005, *MNRAS*, 363, 1069
- Liddle, A.R., & Lyth, D.H. 1992, *Phys. Lett. B*, 291, 391
- Loeb, A., & Rybicki, G.B. 1999, *ApJ*, 524, 527
- Loeb, A., & Zaldarriaga, M. 2004, *Phys. Rev. Lett.* 92, 211301
- Madau, P., Meiksin, A., & Rees, M.J. 1997, *ApJ*, 475, 429, (MMR)

- Magorrian, J., et al. 1998, *AJ*, 115, 2285
- Mo, H., & White, S.D.M. 1996, *MNRAS*, 282, 347
- Mori, M., Umemura, M., & Ferrara, A. 2004, *PASA*, 21, 232
- Navarro, J.F., Frenk, C.S., & White, S.D.M. 1997, *ApJ*, 490, 493
- Oh, S. P. 2001, *ApL*, 553, 499
- Oh, S. P., Nollett, K. M., Madau, P., & Wasserburg, G. J. 2001, *ApL*, 562, L1
- Peebles, P.J.E. 1969, *ApJ*, 155, 393
- Peebles, J.P.E. 1993, “Physical Cosmology”, Princeton University Press.
- Peiris, H.V., et al. 2003, *ApJS*, 148, 213
- Press, W.H., & Schechter, P.L. 1974, *ApJ*, 215, 703
- Pritchard, J.R., & Furlanetto, S.R. 2005, *astro-ph/0508381*
- Qian, Y.-Z. & Wasserburg, G. J. 2002, *ApJ*, 567, 515
- Rappaport, S.A., Podsiadlowski, Ph., & Pfahl, E. 2005, *MNRAS*, 356, 401
- Ricotti, M., & Ostriker, J.P. 2004, *MNRAS*, 352, 547
- Rottgering, H. 2003, *astro-ph/0309537*
- Santos, M.G., Cooray, A., & Knox, L. 2005, *ApJ*, 625, 575
- Schaerer, D. 2002, *A&A*, 382, 28
- Scott, D., & Rees, M.J. 1990, *MNRAS*, 247, 510
- Sheth, R.K., & Tormen, G. 1999, *MNRAS*, 308, 119
- Shull, J.M., & Van Steenberg, M.E. 1985, *ApJ*, 298, 268
- Spergel, D.N., et al. 2003, *ApJS*, 148, 175
- Steinmetz, M., & Bartelmann, M. 1995, *MNRAS*, 272, 570
- Sutherland, R.S., & Dopita, M.A. 1993, *ApJS*, 88, 253
- Tan, J.C., & McKee, C.F. 2004, *ApJ*, 603, 383

- Tumlinson, J., Venkatesan, A., & Shull, J. M. 2004, *ApJ*, 612, 602
- Ueda, H., Shimasaku, K., Sugihara, T., & Suto, Y. 1994, *PASJ*, 46, 319
- Umeda, H. & Nomoto, K. 2003, *Nature*, 422, 871
- Upadhye, A., Ishak, M., & Steinhardt, P.J. 2005, *Phys. Rev. D*, 72, 063501
- Wang, X., Tegmark, M., Santos, M., & Knox, L. 2005, *astro-ph/0501081*
- White, S.D.M. 1984, *ApJ*, 286, 38
- Wouthuysen, S. 1952, *AJ*, 57, 31
- Yu, Q., & Tremaine, S. 2002, *MNRAS*, 335, 965
- Zaldarriaga, M., Furlanetto, S.R., & Hernquist, L. 2004, *ApJ*, 608, 622
- Zygelman, B. 2005, *ApJ*, 622, 1356